Springtime ENSO phase evolution and its relation to rainfall in the continental U.S.

Sang-Ki Lee[1,2], Brian E. Mapes[3], Chunzai Wang[2], David B. Enfield[1,2] and Scott J. Weaver[4]

[1]Cooperative Institute for Marine and Atmospheric Studies, University of Miami, Miami FL

[2]Atlantic Oceanographic and Meteorological Laboratory, NOAA, Miami FL

[3]Rosenstiel School of Marine and Atmospheric Sciences, University of Miami, Miami, Florida

[4]Climate Prediction Center, NOAA, College Park, MD

Revised and submitted to Geophysical Research Letters

February 2014

Corresponding author address: Dr. Sang-Ki Lee, CIMAS, University of Miami, 4600 Rickenbacker Causeway, Miami, FL 33149, USA. E-mail: Sang-Ki.Lee@noaa.gov.

Abstract

Springtime ENSO phase evolution and associated U.S. rainfall variability is explored by performing composite analysis of observational data. Although the tropical Pacific ENSO SST anomalies are weaker and less coherent in boreal spring compared to those in winter, there are unique and significant patterns of U.S. rainfall anomalies frequently appearing during the onset and decay phases of ENSO. In early spring of a decaying El Niño, the atmospheric jet stream and associated storm track shift southward, causing more frequent wet conditions across the southern U.S. and dry conditions in a belt south and east of the Ohio River. In late spring of a developing El Niño, synoptic activity over the U.S. reduces overall and the southwesterly low-level winds that carry moist air from the Gulf of Mexico to the U.S. shift westward, causing a similar dipole of rainfall anomalies between the southern U.S. and the Ohio Valley.

1. Introduction

The El Niño - Southern Oscillation (ENSO) is the dominant source of interannual climate variability in the United States [e.g., *Ropelewski and Halpert*, 1986]. Although it can develop and dissipate at any time in a given year, it is usually tightly phase locked to the seasonal cycle with a strong tendency to have the peak phase during boreal winter [*Rasmusson and Carpenter*, 1982] - see *Wang and Picaut* [2004] for a review of the seasonal phase locking mechanisms of ENSO. Due to both the seasonal phase locking of the ENSO sea surface temperature (SST) anomalies and the seasonal cycle of the atmospheric background state, the remote influence of ENSO on the U.S. climate is also strongest in the winter [e.g., *Horel and Wallace*, 1981; *Barnston and Livezey*, 1987].

Shortly after reaching its peak in boreal winter, an ENSO event usually decays rapidly in spring. During this time, the ENSO SST anomalies in the tropical Pacific are typically much weaker in amplitude, while their spatial structure becomes much less coherent; thus the correlation between ENSO and the U.S. climate starts to break down after late winter or early spring [e.g., *Mo*, 2010]. Indeed, as shown in Figure 1a and 1b, the ENSO composite SST anomalies in the eastern Pacific (120Wº – 80Wº and 5Sº – 5Nº; EP hereafter) terminate rather abruptly and almost completely dissipate by March (+1) or April (+1) - any month in an ENSO onset year is identified by suffix (0) whereas any month in ENSO decay year is denoted by suffix (+1) hereafter. Interestingly, the SST anomalies in the central Pacific (180Eº – 120Wº and 5Sº – 5Nº; CP hereafter) weaken much more gradually and persist throughout the spring until around June (+1). As a result, a zonal gradient of SST anomalies tends to form along the equatorial Pacific between CP and EP during the decay phase of ENSO.

Every ENSO event is somewhat different from others [*Trenberth and Stepaniak,* 2001] - see Figure S1 and S2 in the auxiliary material for time-longitude plots of all ENSO events that occurred during 1949 - 2012. This is especially true during the springtime ENSO phase evolution. As shown in Figure 1c and 1d, the composite standard deviation of the tropical Pacific SST anomalies in spring is quite small in CP but much larger in EP, indicating that while the ENSO SST anomalies in spring are relatively robust in CP, those in EP are highly inconsistent between ENSO events, especially during the decay of El Niño and onset of La Niña. During the decay phase, the SST anomalies in EP often switch to the opposite sign producing a zonal seesaw pattern between CP and EP (e.g., 1965-1966 El Niño; 2007-2008 La Niña). In some cases, the SST anomalies in CP and EP dissipate together during or after spring (e.g., 1991-1992 El Niño; 1988-1989 La Niña), or further evolve into the onset of another ENSO event with either the same or opposite sign in the subsequent months (e.g., 1986-1987 El Niño; 1964-1965 La Niña). In rare cases, the SST anomalies in EP persist much longer than those in CP, as reported for the decay of the two extreme El Niños in 1982-1983 and 1997-1998 [*Lengaigne and Vecchi*, 2009]. During the onset phase, both the SST anomalies in CP and the zonal gradient of SST anomalies between CP and EP are generally weaker (see Figure 1a and 1b). As shown in Figure 1c and 1d, event-to-event variability of ENSO SST anomalies in EP is very large during the onset phase in agreement with earlier studies [e.g., *Wang*, 1995; *Fedorov and Philander,* 2000; *McPhaden and Zhang*, 2009].

Since atmospheric convection is more sensitive to the SST anomalies in CP than in EP (due to larger absolute SSTs in CP than in EP), and the atmospheric background state in spring allows tropical forcing of extra-tropical stationary waves in the Northern Hemisphere [*Lee et al*., 2009; 2013; *Jin and Kirtman*, 2009], it is likely that the relatively coherent SST anomalies in CP during the onset and decay phases can excite ENSO teleconnection patterns to influence climate variability in the U.S. Given that severe weather events (i.e., tornadoes, hail, thunderstorms and heavy precipitation) frequently occur in spring over the U.S., it is important to explore whether the tropical Pacific SST anomalies appearing during the springtime ENSO phase evolution are linked to any repeating pattern of climate anomalies over the U.S. The main objective of the present study is to explore this question. Our strategy here is to perform composite analysis of the tropical Pacific SST and U.S. rainfall anomalies for the onset versus decay phases. We also analyze two special cases, which cannot be solely characterized as either onset or decay phase. These cases occur when the decay of an ENSO event is immediately followed by the onset of another ENSO event with either the opposite or same sign. The former is referred to here as the transition phase and the latter as the resurgence phase.

2. Data and Methods

We use the Extended Reconstructed Sea Surface Temperature version 3b (ERSST3), a blended satellite and in situ analysis of global monthly SST on a 2^{o} longitude by 2^{o} latitude grid for the period of 1949 – 2012. The CPC unified gauge-based analysis of U.S. daily precipitation is used to derive monthly rainfall over the U.S. for 1949 – 2012 [*Higgins et al*., 1996]. This dataset is based on about 8,000 - 13,000 station reports each day, quality controlled to eliminate duplicates and overlapping stations, and gridded on 0.25^{o} longitude by 0.25^{o} latitude grid. The NCEP-NCAR reanalysis for the same period is used to derive monthly moisture transport, precipitable water content, variance of 5-day high-pass filtered meridional winds at 300 hPa, and geopotential height at 850 hPa.

We perform composite analysis of the tropical Pacific SST and U.S. rainfall anomalies for the onset and decay phases of ENSO, and also for the two mixed cases of transition and resurgence phases. Using the threshold for ENSO that three-month averaged SST anomalies in Niño 3.4 (120Wº – 170Wº and 5Sº – 5Nº) should exceed 0.5°C for a minimum of five consecutive months, 21 El Niño and 22 La Niña events are identified during the period of 1949 – 2012 (Table S1). Note that multi-year ENSO events are treated as multiple ENSO events. For instance, the La Niña event that started in the summer of 1998 and continued until the spring of 2001 is treated here as three consecutive La Niña events (i.e., 1998-1999, 1999-2000, and 2000-2001).

The composite mean differences of SST and U.S. rainfall anomalies between the 21 El Niño and 22 La Niña events (i.e., 0.5 × [<El Niño> - <La Niña>], where < > represents composite mean) are analyzed focusing on their onset and decay phases in boreal spring. Student-*t* tests (two-tailed) are performed to determine statistical significance of the composite mean differences. By using the composite mean differences, the focus is on the results and interpretations pertaining to both El Niño and La Niña with reversed sign. In the following sections, three U.S. regions, namely the South, Central and Southeast U.S. as defined by National Climate Data Center (see Figure S3), are frequently referred to describe regional U.S. rainfall anomalies.

3. Onset and Decay Phases

As shown in Figure 1a and 1b, the ENSO SST anomalies in the tropical Pacific evolve rapidly in spring. Therefore, the ENSO composite mean differences of SST anomalies during the onset and decay phases are shown separately for early (March – mid-April) and late (mid-April –

May) spring in Figure 2a-d. During the onset phase, the tropical Pacific SST anomalies are quite weak in early spring, but grow rapidly and achieve a statistically significant pattern in late spring that is similar to the canonical ENSO pattern (i.e., warm SST anomalies in both CP and EP). During the decay phase, on the other hand, the ENSO SST anomalies remain strong in early spring especially in CP, but decay rapidly afterward. In late spring, the SST anomalies in CP largely drop below 0.5ºC. It is interesting to note that the spatial pattern of SST anomalies during the decay phase resembles the 2nd Empirical Orthogonal Function pattern of the tropical Pacific SST anomalies, also referred to as Trans-Niño, central Pacific El Niño, El Niño Modoki, and warm pool El Niño in the literature [e.g., *Trenberth and Stepaniak*, 2001; *Yeh et al*., 2009; *Ashok et al*., 2007; *Kug et al*., 2009].

Consistent with the rapidly evolving springtime ENSO SST anomalies in the tropical Pacific, the associated U.S. rainfall anomalies also evolve considerably in spring (Figure 2e-h). During the onset phase, U.S. rainfall anomalies are only weakly affected in early spring, consistent with the small amplitude of ENSO SST anomalies in that period. In late spring of a developing El Niño, the South U.S., especially Texas, experiences wet conditions, while the Ohio Valley experiences dry conditions.

During the decay phase, U.S. rainfall anomalies are quite significant in early spring, consistent with the large amplitude ENSO SST anomalies in that period. For a decaying El Niño, the Great Plains and the Southeast U.S., particularly Florida, as well as the southwestern U.S. experience wet conditions, while the regions immediately south and east of the Ohio River including Tennessee, Kentucky, and West Virginia experience dry conditions. Note that a similar spatial pattern of U.S. rainfall anomalies occurs during the peak of El Niño in boreal winter [e.g., Mo, 2010]. Consistent with the small amplitude of ENSO SST anomalies in late spring of the decay phase, U.S. rainfall anomalies are relatively small and insignificant during that period.

4. Transition and Resurgence Phases

For some ENSO events, the ENSO phase evolutions in spring cannot be solely characterized as either an onset or a decay phase because the decay of an ENSO event is often accompanied by the onset of another ENSO event with either the opposite or same sign. The former is referred to here as the transition phase and the latter as the resurgence phase. Yu and Kim [2010] argued that an El Niño-to-La Niña transition is more likely to occur when the mean equatorial Pacific thermocline is shallower than normal whereas a resurgence of El Niño is more likely when the mean equatorial Pacific thermocline is deeper than normal. However, further study is needed to explore whether the same mechanism applies to the La Niña-to-El Niño transition and La Niña resurgence, which is beyond the scope of this study.

The spring of 1988, for example, is an El Niño-to-La Niña transition phase because it is both the decay phase of the 1987-1988 El Niño and the onset phase of the 1988-1989 La Niña. Another example is the spring of 1999, which is a resurgence phase of La Niña because it is both the decay phase of the 1998-1999 La Niña and the onset phase of the 1999-2000 La Niña. As summarized in Table S1, eleven El Niño-to-La Niña transition phases, six La Niña-to-El Niño transition phases, four resurgence phases of El Niño, and ten resurgence phases of La Niña are identified during the period of 1949 - 2012.

The ENSO composite mean differences of SST anomalies during the transition (0.5 × [<El Niño-to-La Niña transition> - <La Niña-to-El Niño transition>]) and resurgence (0.5 × [<El Niño resurgence> - <La Niña resurgence>]) phases are shown for early and late spring in Figure 3a-d.

As in the previous section, the focus is on the results and interpretations specific to the El Niño-to-La Niña transition and El Niño resurgence but applicable to the La Niña-to-El Niño transition and La Niña resurgence, respectively, with reversed sign. During the El Niño-to-La Niña transition phase, the warm SST anomalies in CP decay rapidly, while the cold SST anomalies in EP quickly emerge in late spring and achieve below -0.5ºC in the far eastern equatorial Pacific. This suggests that, during the El Niño-to-La Niña transition phase, the tropical Pacific SST anomalies in late spring are typically under the influence of the onset phase of the succeeding La Niña. During the El Niño resurgence phase, the warm SST anomalies are relatively strong and significant throughout spring especially in CP.

As shown in Figure 3e and 3f, during the El Niño-to-La Niña transition phase, the spatial pattern of U.S. rainfall anomalies in early spring is somewhat similar to that in early spring of a decaying El Niño, although the amplitude is much smaller overall (compare Figure 3e with Figure 2g). In late spring, the weakly wet conditions in the South U.S. switch to very dry conditions, and the regions immediately east and south of the lower Mississippi and Ohio Rivers including Mississippi, Tennessee and Kentucky are quite wet. Thus, a nearly reversed spatial pattern (i.e., wet South U.S. and dry Ohio Valley) occurs in late spring of a developing El Niño (Figure 2f), suggesting that the anomalous U.S. rainfall pattern shown in Figure 3f can be attributed to the developing La Niña.

During the resurgence phase of El Niño, U.S. rainfall anomalies are relatively strong in both early and late spring (Figure 3g and 3h), consistent with the strong tropical Pacific SST anomalies during that time (Figure 3c and 3d). However, they are statistically significant only in limited areas, likely because the resurgence of El Niño took place only four times during 1949-2012. The spatial pattern of U.S. rainfall anomalies in early spring is similar to that in early spring of a decaying El Niño (compare Figure 3g with Figure 2g), suggesting that the anomalous U.S. rainfall pattern in that period can be attributed to the decaying El Niño. In late spring, the South U.S. is anomalously wet, while the Central U.S. including Alabama, Missouri and Illinois are anomalously dry (Figure 3h). This spatial pattern of U.S. rainfall anomalies in late spring suggests that the anomalous U.S. rainfall pattern in that period can be attributed to the developing El Niño (compare Figure 3h with Figure 2f).

5. Springtime Atmospheric Anomalies over the U.S. associated with ENSO

In an attempt to explain the atmospheric dynamics linking the springtime ENSO phase evolution to U.S. rainfall anomalies, we perform composite analysis of the anomalous moisture transport, precipitable water content, variance of 5-day high-pass filtered meridional winds at 300 hPa, which is used to measure extratropical storm activity, and geopotential height at 850 hPa for the onset and decay phases of ENSO. We focus mainly on late spring of the onset phase and early spring of the decay phase because the corresponding U.S. rainfall anomalies are relatively strong and significant.

It is well known that El Niño events cause the winter atmospheric jet stream to strengthen over the central and eastern North Pacific and to take a more direct path to North America as opposed to its usual wavy northeastward path. Thus, the winter storm track over the U.S. generally shifts southward, causing more frequent wet conditions in the southern U.S. and northern Mexico and dry conditions in the Ohio Valley [e.g., *Ropelewski and Halpert*, 1986; *Eichler and Higgins*, 2006; *Mo*, 2010]. As shown in Figure 4a (contours), during the decay phase of El Niño, the extratropical storm track is shifted southward in early spring (i.e., synoptic activity decreases over the northern and central U.S. and increases over the southern U.S. and northern Mexico), suggesting that the mechanism through which ENSO affects U.S. rainfall in winter months still prevails in early spring. The moisture transport and precipitable water content anomalies are consistent with the southward shift of the atmospheric jet stream (Figure 4c).

In late spring of a developing El Niño, synoptic activity over the U.S. reduces overall (contours in Figure 4d). However, there is no apparent southward shift of the extratropical storm tracks (i.e., synoptic activity decreases over the U.S. but does not increase south of the U.S.). Instead, an anomalous low-level anticyclone that forms east of the Rockies suppresses the southwesterly low-level winds (Figure 4d) that carry moist air from the Gulf to the Central U.S., and redirects the moisture transport to the South U.S. (Figure 4f), in agreement with the increased instability (i.e., reduced lifted index; not shown) and amount of total precipitable water (Figure 4f) over the South U.S and the Gulf coast region. These features in the atmospheric anomalies are consistent with the dipole of rainfall anomalies shown in Figure 2f: anomalously wet in the South U.S. and dry in the Ohio River. The overall spatial patterns of the atmospheric anomalies for the transition and resurgence phases can be similarly explained as those for the onset and decay phases (Figure S4).

6. Summary and Discussion

This study explores various types of springtime ENSO phase evolution and associated rainfall variability in the continental U.S. In boreal spring, the ENSO SST anomalies in the tropical Pacific are weaker and less coherent compared to those in winter. Nevertheless, there are unique and significant patterns of springtime U.S. rainfall anomalies frequently appearing during the onset and decay phases of ENSO, and also during the two mixed cases of transition and resurgence phases. These patterns of rainfall anomalies are forced by the meridional shift of the atmospheric jet stream and extratropical storm tracks, the zonal shift and strengthening/weakening of the moisture transport from the Gulf of Mexico, and the changes in the atmospheric stability and moisture availability.

Note that these atmospheric anomalies are direct results of springtime ENSO teleconnections, which are potentially predictable [e.g., *Quan et al*. 2006]. However, given that our current understanding of the springtime ENSO phase evolution and the associated atmospheric teleconnection patterns are very poor, coordinated and comprehensive research efforts are needed to achieve useful seasonal forecast skill for U.S. rainfall during the springtime ENSO phase evolution.

Among others, one limitation of this study is in our assumption that the results specific to El Niño can be applied to La Niña with reversed sign. Although this assumption is valid as the first approximation (not shown), there exist El Niño - La Niña asymmetry and nonlinearity of teleconnections in spring [e.g., *Jin et al*., 2003; *Hoerling et al*., 1997]. This is an important subject that should be fully explored in future studies along with other important aspects not explicitly included in this study such as the signal to noise ratio in springtime U.S. rainfall [e.g., *Hoerling and Kumar*, 1997] and the predictability of the springtime ENSO phase evolution.

Acknowledgments. We would like to thank two anonymous reviewers, Greg Foltz and Libby Johns for their thoughtful comments and careful reviews. This work was supported by NOAA Climate Program Office through its MAPP program [Grant# NA12OAR4310083]. BEM acknowledges support by NSF [Grant# 0731520] and ONR [Grant# N000141310704].

References

Ashok, K., S. Behera, A. S. Rao, H. Y. Weng, and T. Yamagata, 2007: El Niño Modoki and its possible teleconnection, *J. Geophys. Res*., 112, C1107, doi:10.1029/2006JC003798.

Barnston A. G., and R. E. Livezey, 1987: Classification, seasonality, and persistence of low-frequency atmospheric circulation patterns. *Mon. Wea. Rev*., **115**, 1,083–1,126.

Eichler, T, and W. Higgins, 2006: Climatology and ENSO-related variability of North American extratropical cyclone activity. *J. Clim.*, **19**, 2076–2093.

Fedorov, A. V., and S. G. Philander, 2000: Is El Niño Changing? *Science*, **288**, 1997-2002.

Higgins, R. W., K. C. Mo, and S. D. Schubert, 1996: The moisture budget of the central United States in spring as evaluated in the NCEP/NCAR and the NASA/DAO reanalyses. *Mon. Wea. Rev*., **124**, 939–963.

Hoerling, M. P., A. Kumar, and M. Zhong, 1997: El Niño, La Niña, and the nonlinearity of their teleconnections. *J. Clim.*, **10**, 1769–1786.

Hoerling, M. P., and A. Kumar, 1997: Why do North American climate anomalies differ from one El Niño event to another? *Geophys. Res. Lett*., **24**, 1059–1062.

Horel, J. D., and J. M. Wallace, 1981: Planetary-scale atmospheric phenomena associated with the Southern Oscillation. *Mon. Wea. Rev.* **109**, 813–829.

Jin, D., and B. P. Kirtman, 2009: Why the Southern Hemisphere ENSO responses lead ENSO, *J. Geophys. Res*., **114**, D23101, doi:10.1029/2009JD012657.

Jin, F.-F., S.-I. An, A. Timmermann, and J. Zhao, 2003: Strong El Niño events and nonlinear dynamical heating, *Geophys. Res. Lett*., **30**, 1120, doi:10.1029/2002GL016356.

Kug, J.-S., F.-F. Jin, and S.-I. An, 2009: Two types of El Niño events: cold tongue El Niño and warm pool El Niño. *J. Clim.*, **22**, 1,499–1,515.

Lengaigne, M., and G. A. Vecchi, 2009: Contrasting the termination of moderate and extreme El Niño events in Coupled General Circulation Models. *Clim. Dyn.*, **35**, 299–313.

Lee, S.-K., C. Wang, and B. E. Mapes, 2009: A simple atmospheric model of the local and teleconnection responses to tropical heating anomalies. *J. Clim*., **22**, 272-284.

Lee, S.-K., R. Atlas, D. B. Enfield, C. Wang, and H. Liu, 2013: Is there an optimal ENSO pattern that enhances large-scale atmospheric processes conducive to major tornado outbreaks in the U.S.? *J. Clim.*, **26**, 1,626-1,642.

McPhaden, M. J., and X. Zhang, 2009: Asymmetry in zonal phase propagation of ENSO sea surface temperature anomalies, *Geophys. Res. Lett.*, **36**, L13703, doi:10.1029/2009GL038774.

Mo, K. C., 2010: Interdecadal modulation of the impact of ENSO on precipitation and temperature over the United States. *J. Clim*., **23**, 3639–3656.

Quan, X., M. Hoerling, J. Whitaker, G. Bates, and T. Xu, 2006: Diagnosing sources of U.S. seasonal forecast skill. *J. Clim*., **19**, 3279–3293

Rasmusson, E. M., and T. H. Carpenter, 1982: Variations in tropical sea surface temperature and surface wind fields associated with the Southern Oscillation/El Niño. *Mon. Wea. Rev.*, **110**, 354-384.

Ropelewski, C. F., and M. S. Halpert, 1986: North American precipitation and temperature patterns associated with the El Nino/ Southern Oscillation (ENSO). *Mon. Wea. Rev.*, **114**, 2,352-2,362.

Trenberth, K. E., and D. P. Stepaniak, 2001: Indices of El Niño evolution, *J. Clim.*, **14**, 1697–1701.

Wang, B., 1995: Interdecadal changes in El Niño onset in the last four decades. *J. Clim.*, **8**, 267–285.

Wang, C., and J. Picaut, 2004: Understanding ENSO physics - A review. In: Earth's Climate: The Ocean-Atmosphere Interaction. C. Wang, S.-P. Xie, and J. A. Carton, Eds., AGU Geoph. Monog. Series, **147**: 21-48.

Yeh, S.-W., J.-S. Kug, B. Dewitte, M.- H. Kwon, B. Kirtman, and F.-F. Jin, 2009: El Niño in a changing climate, *Nature*, 461, 511-514.

Yu, J.-Y., and S. T. Kim, 2010: Three evolution patterns of Central-Pacific El Niño, *Geophys. Res. Lett.*, **37**, L08706, doi:10.1029/2010GL042810.

Figure captions

Figure 1. Time-longitude plots of composite (a and b) means and (c and d) standard deviations of the tropical Pacific SST anomalies averaged between 5°S and 5°N for (a and c) 21 El Niños and (b and d) 22 La Niñas during 1949-2012, derived from ERSST3. The composite standard deviation of El Niño (La Niña) measures the spread of the 21 El Niños (22 La Niñas) from their composite mean. The horizontal black line marks the last day of Year (0). The horizontal gray lines indicate the start (March 1) and end (May 30) dates of boreal spring. The unit is °C.

Figure 2. Composite mean differences of (a - d) SST and (e - h) U.S. rainfall anomalies between the onset phase of El Niño and La Niña in (a, e) early spring and (b, f) late spring; and between the decay phase of El Niño and La Niña in (c, g) early spring and (d, h) late spring derived from ERSST3 and CPC unified gauge-based analysis of U.S. daily precipitation. In (a – c), negative and positive contours are in blue and red, respectively, whereas the zero-contour is in dashed

black. In (d - f), negative and positive contours are in brown and green, respectively. Significant values at 90% or above based on a student-*t* test (two-tailed) are shaded. The unit is °C for the SST anomalies and mm·day^{-1} for the rainfall anomalies.

Figure 3. Composite mean differences of (a - d) SST and (e - h) U.S. rainfall anomalies between the El Niño-to-La Niña transition phase and the La Niña-to-El Niño transition phase in (a, e) early spring and (b, f) late spring; and between the resurgence phase of El Niño and the resurgence phase of La Niña in (c, g) early spring and (d, h) late spring derived from ERSST3 and CPC unified gauge-based analysis of U.S. daily precipitation. In (a – c), negative and positive contours are in blue and red, respectively, whereas the zero-contour is in dashed black. In (d - f), negative and positive contours are in brown and green, respectively. Significant values at 90% or above based on a student-*t* test (two-tailed) are shaded. The unit is °C for the SST anomalies and mm·day^{-1} for the rainfall anomalies.

Figure 4. Upper-panel: anomalous geopotential height at 850 hPa (color shades) and variance of 5-day high-pass filtered meridional winds at 300 hPa (contours) for (a) early spring of ENSO decay phase and (d) late spring of ENSO onset phase. Mid-panel: climatological moisture transport (vectors) and precipitable water (color shades) in (b) early and (e) late spring. Bottom-panel: anomalous moisture transport (vectors) and precipitable water (color shades) for (c) early spring of ENSO decay phase and (f) late spring of ENSO onset phase. The units are kg·m^{-1}·s^{-1} for moisture transport, kg·m^{-2} for precipitable water, gpm for geopotential height and m^{2}·s^{-2} for variance of meridional winds.

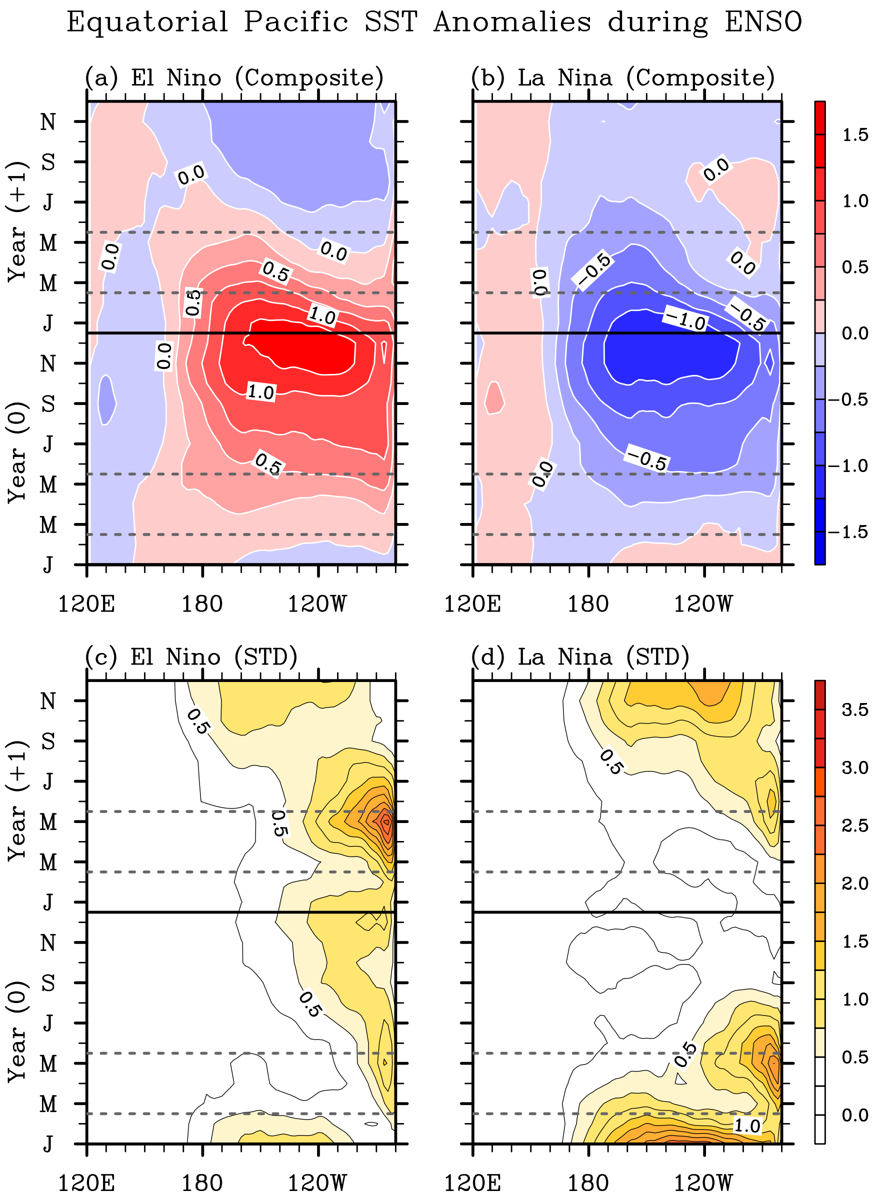

Figure 1. Time-longitude plots of composite (a and b) means and (c and d) standard deviations of the tropical Pacific SST anomalies averaged between 5°S and 5°N for (a and c) 21 El Niños and (b and d) 22 La Niñas during 1949-2012, derived from ERSST3. The composite standard deviation of El Niño (La Niña) measures the spread of the 21 El Niños (22 La Niñas) from their composite mean. The horizontal black line marks the last day of Year (0). The horizontal gray lines indicate the start (March 1) and end (May 30) dates of boreal spring. The unit is °C.

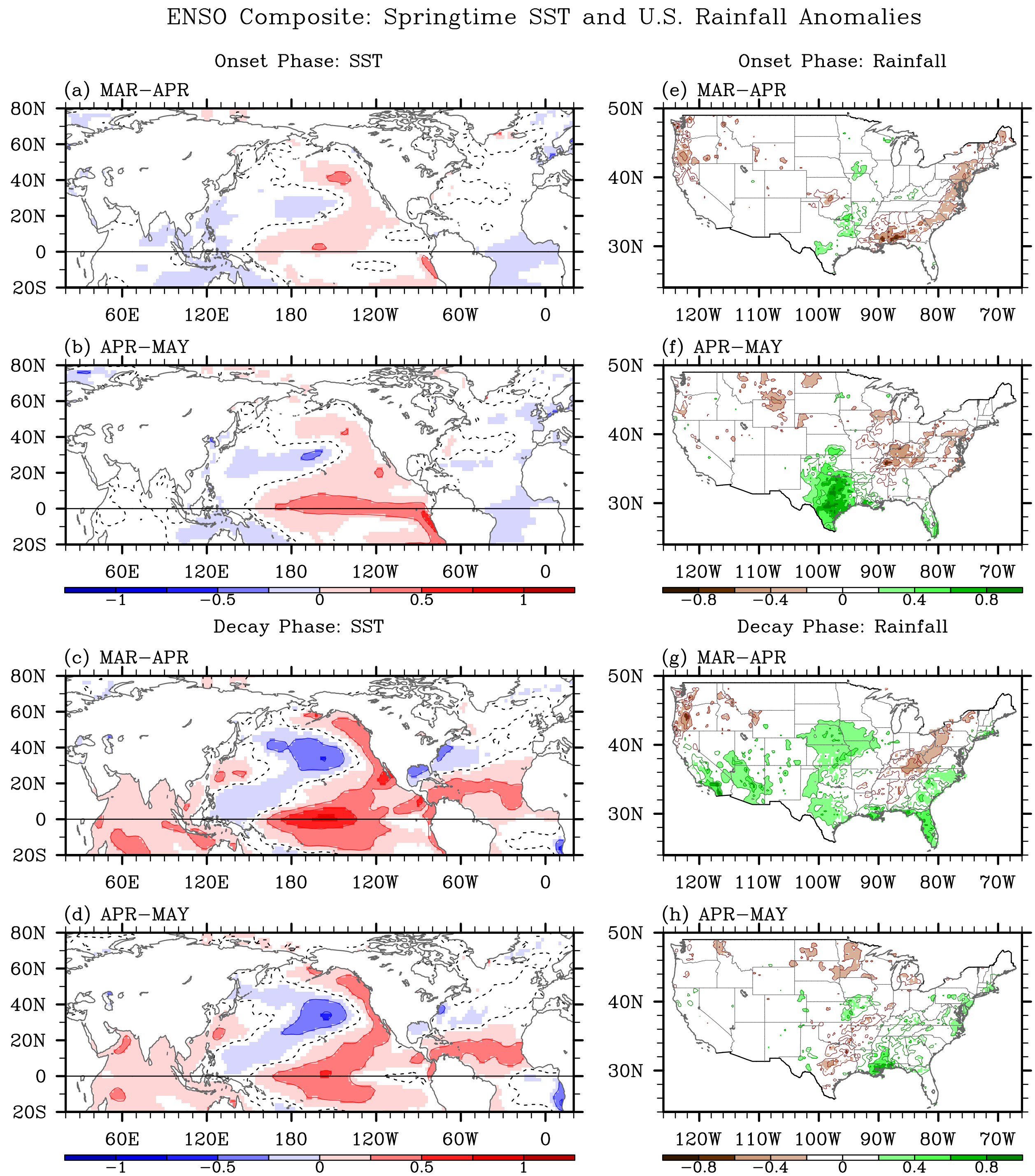

Figure 2. Composite mean differences of (a - d) SST and (e - h) U.S. rainfall anomalies between the onset phase of El Niño and La Niña in (a, e) early spring and (b, f) late spring; and between the decay phase of El Niño and La Niña in (c, g) early spring and (d, h) late spring derived from ERSST3 and CPC unified gauge-based analysis of U.S. daily precipitation. In (a – c), negative

and positive contours are in blue and red, respectively, whereas the zero-contour is in dashed black. In (d - f), negative and positive contours are in brown and green, respectively. Significant values at 90% or above based on a student-*t* test (two-tailed) are shaded. The unit is °C for the SST anomalies and $mm \cdot day^{-1}$ for the rainfall anomalies.

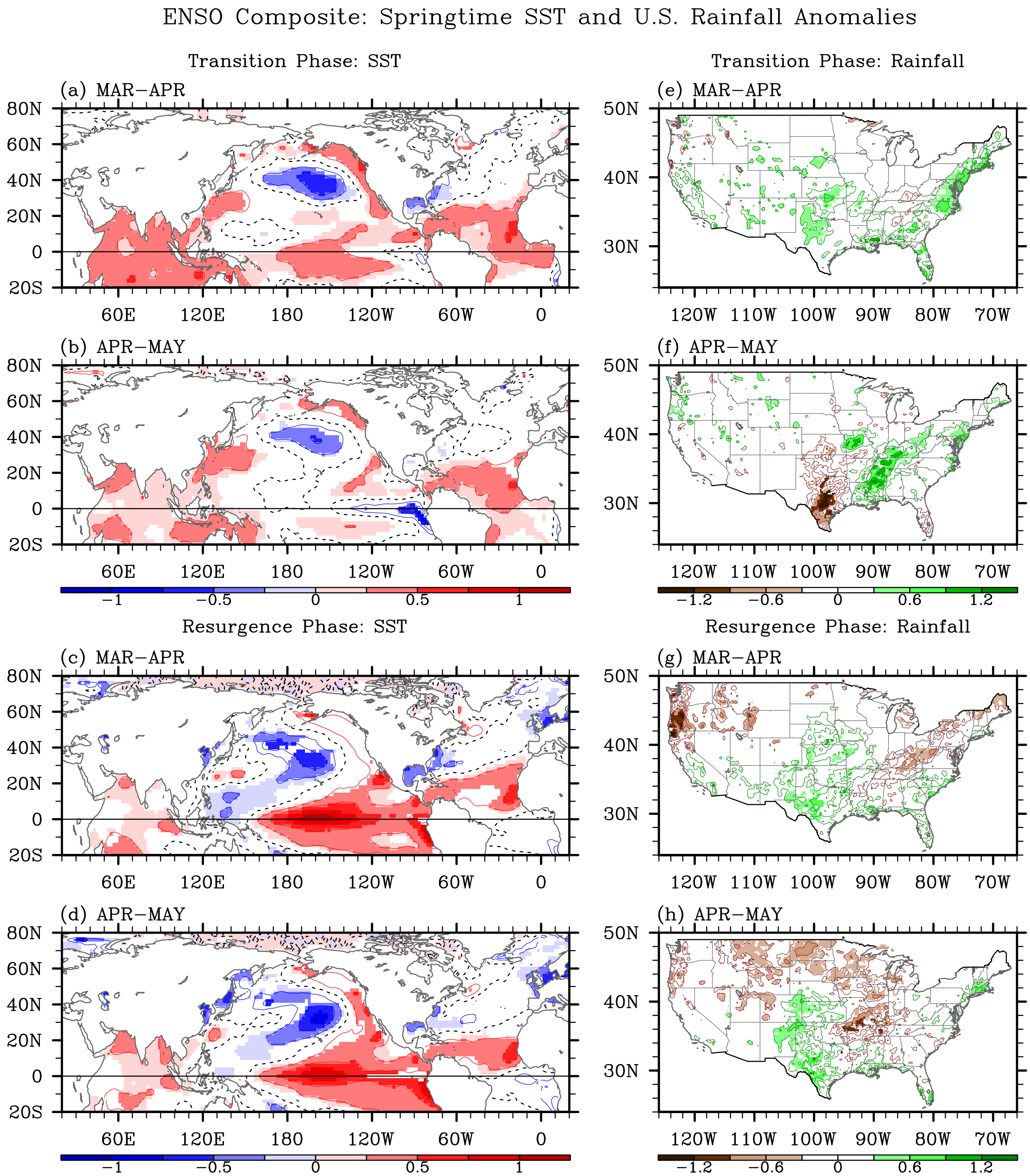

Figure 3. Composite mean differences of (a - d) SST and (e - h) U.S. rainfall anomalies between the El Niño-to-La Niña transition phase and the La Niña-to-El Niño transition phase in (a, e) early spring and (b, f) late spring; and between the resurgence phase of El Niño and the resurgence phase of La Niña in (c, g) early spring and (d, h) late spring derived from ERSST3

and CPC unified gauge-based analysis of U.S. daily precipitation. In (a – c), negative and positive contours are in blue and red, respectively, whereas the zero-contour is in dashed black. In (d - f), negative and positive contours are in brown and green, respectively. Significant values at 90% or above based on a student-*t* test (two-tailed) are shaded. The unit is °C for the SST anomalies and mm·day^{-1}for the rainfall anomalies.

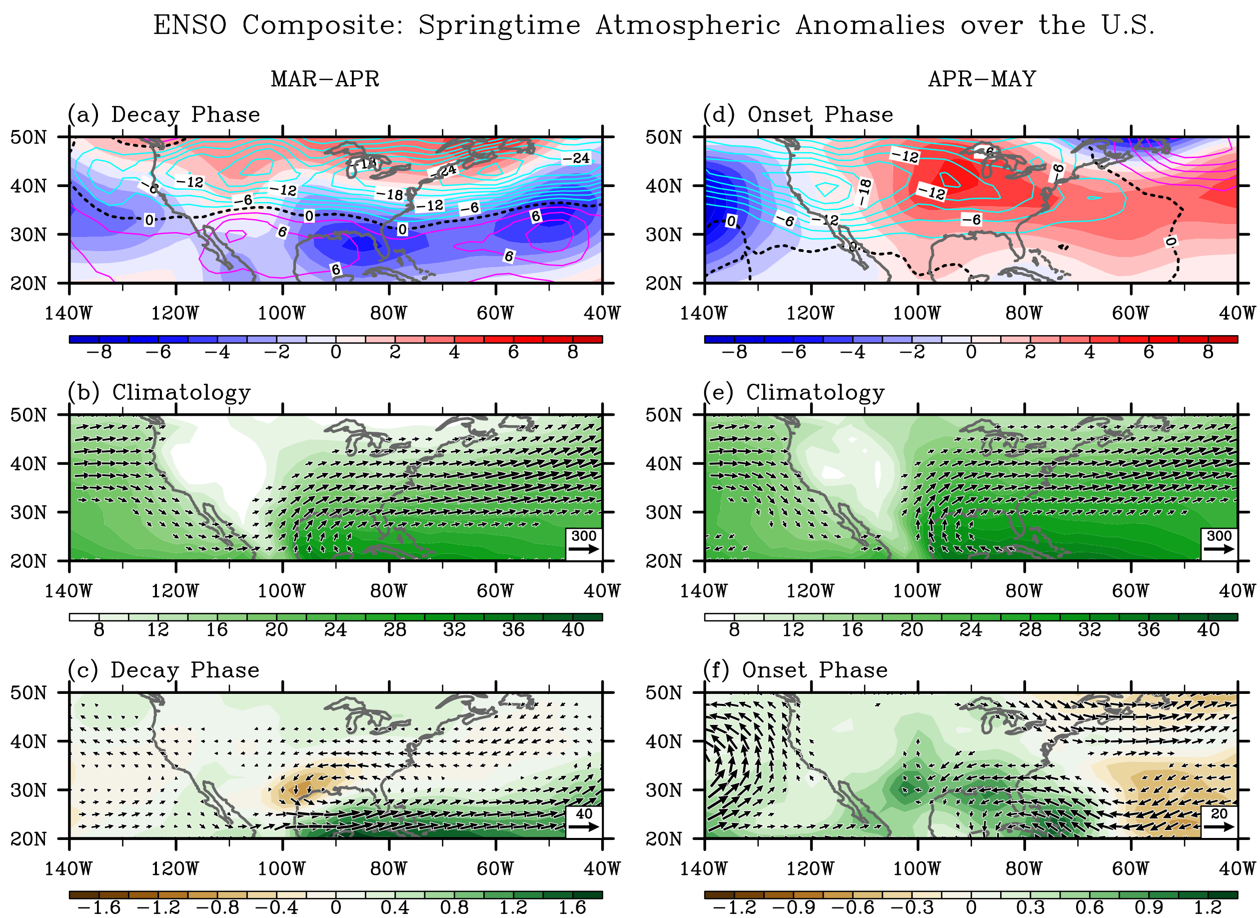

Figure 4. Upper-panel: anomalous geopotential height at 850 hPa (color shades) and variance of 5-day high-pass filtered meridional winds at 300 hPa (contours) for (a) early spring of ENSO decay phase and (d) late spring of ENSO onset phase. Mid-panel: climatological moisture transport (vectors) and precipitable water (color shades) in (b) early and (e) late spring. Bottom-panel: anomalous moisture transport (vectors) and precipitable water (color shades) for (c) early spring of ENSO decay phase and (f) late spring of ENSO onset phase. The units are $kg \cdot m^{-1} \cdot s^{-1}$ for moisture transport, $kg \cdot m^{-2}$ for precipitable water, gpm for geopotential height and $m^2 \cdot s^{-2}$ for variance of meridional winds.

Table S1. 21 El Niños and 22 La Niñas identified during 1949 - 2012 based on the threshold that three-month averaged SST anomalies in Niño 3.4 should exceed 0.5°C for a minimum of five consecutive months. These ENSO events are listed by their onset - decay years (i.e., year (0) - year (+1)). Those ENSO events followed by the onset of another ENSO event of the opposite and same sign during the decay phase are indicated as "Transition" and "Resurgence", respectively, while those dissipated to neutral ENSO conditions are indicated as "Dissipation". ERSST3 is used to compute the SST anomalies in Niño 3.4.

21 El Niños		22 La Niñas	
Year (0) - Year (+1)	Decay phase	Year (0) - Year (+1)	Decay phase
1951 - 1952	Dissipation	1949 - 1950	Resurgence
1953 - 1954	Transition	1950 - 1951	Transition
1957 - 1958	Resurgence	1954 - 1955	Resurgence
1958 - 1959	Dissipation	1955 - 1956	Resurgence
1963 - 1964	Transition	1956 - 1957	Transition
1965 - 1966	Dissipation	1964 - 1965	Transition
1968 - 1969	Resurgence	1970 - 1971	Resurgence
1969 - 1970	Transition	1971 - 1972	Transition
1972 - 1973	Transition	1973 - 1974	Resurgence
1976 - 1977	Resurgence	1974 - 1975	Resurgence
1977 - 1978	Dissipation	1975 - 1976	Transition
1982 - 1983	Transition	1983 - 1984	Resurgence
1986 - 1987	Resurgence	1984 - 1985	Dissipation
1987 - 1988	Transition	1988 - 1989	Dissipation
1991 - 1992	Dissipation	1995 - 1996	Dissipation
1994 - 1995	Transition	1998 - 1999	Resurgence
1997 - 1998	Transition	1999 - 2000	Resurgence
2002 - 2003	Dissipation	2000 - 2001	Dissipation
2004 - 2005	Transition	2005 - 2006	Transition
2006 - 2007	Transition	2007 - 2008	Dissipation
2009 - 2010	Transition	2010 - 2011	Resurgence
		2011 - 2012	Dissipation

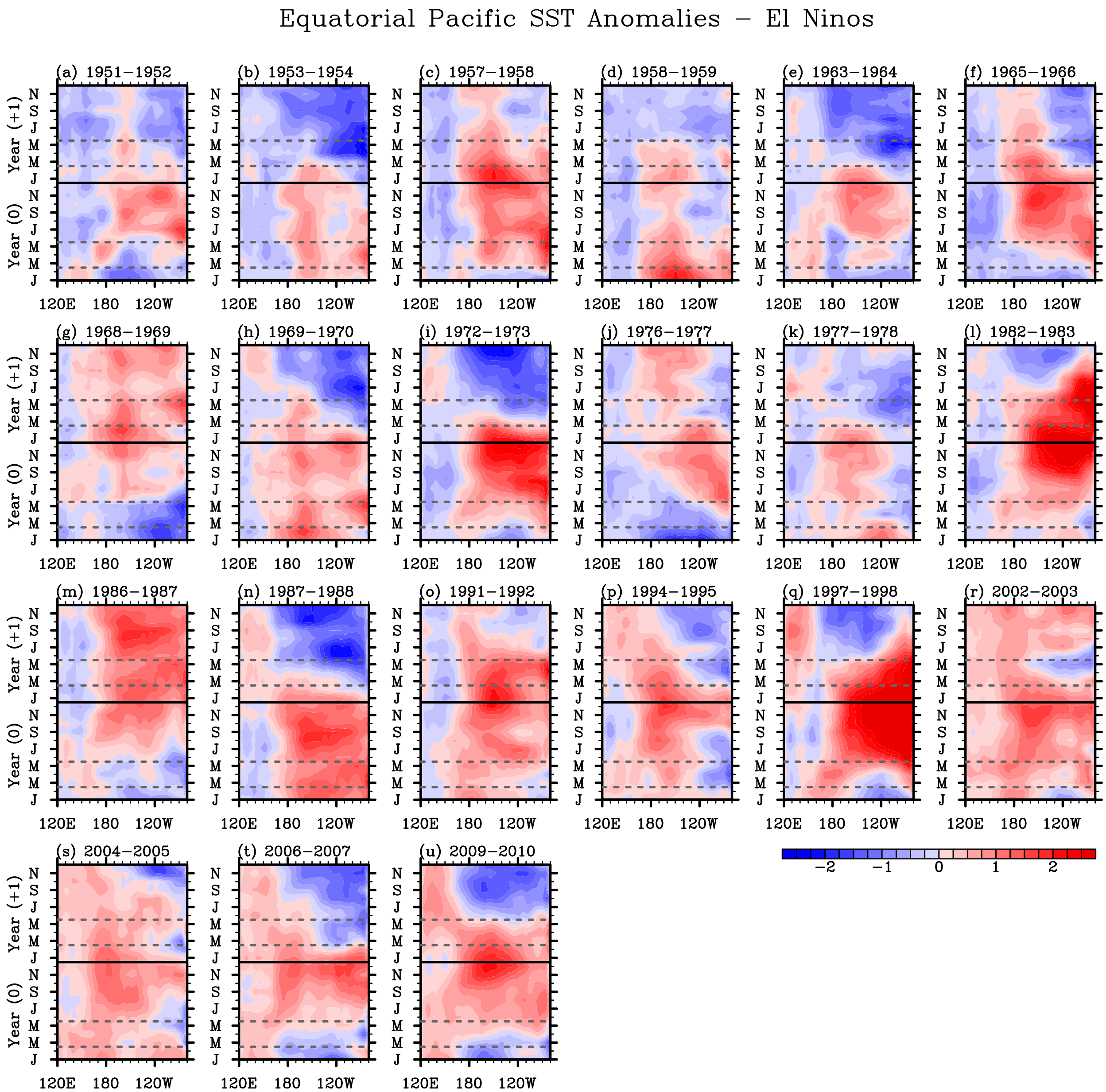

Figure S1. Time-longitude plots of the tropical Pacific SST anomalies averaged between 5°S and 5°N for 21 El Niños that occurred during 1949-2012, derived from ERSST3. The unit is °C.

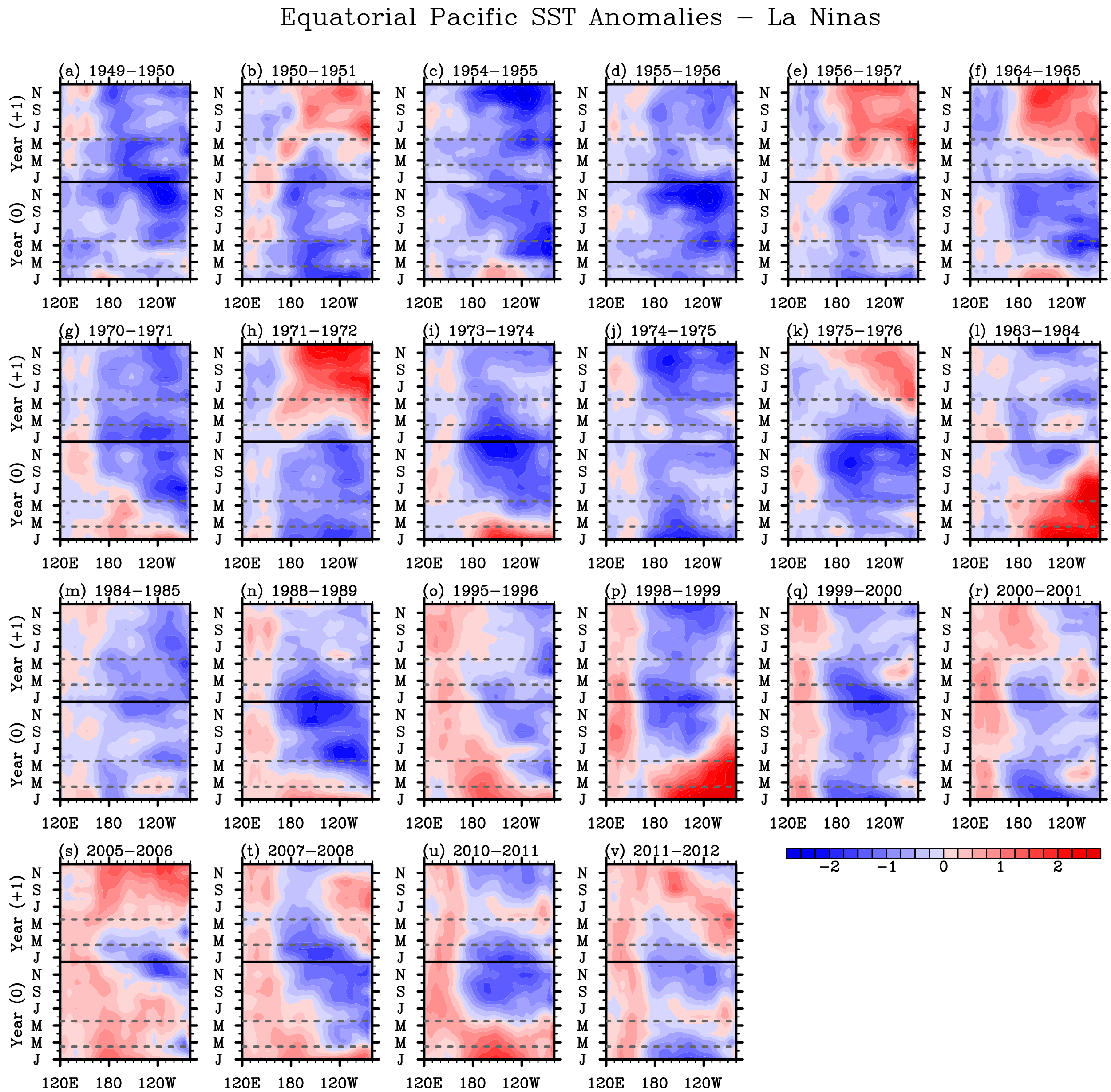

Figure S2. Time-longitude plots of the tropical Pacific SST anomalies averaged between 5°S and 5°N for 22 La Niñas that occurred during 1949-2012, derived from ERSST3. The unit is °C.

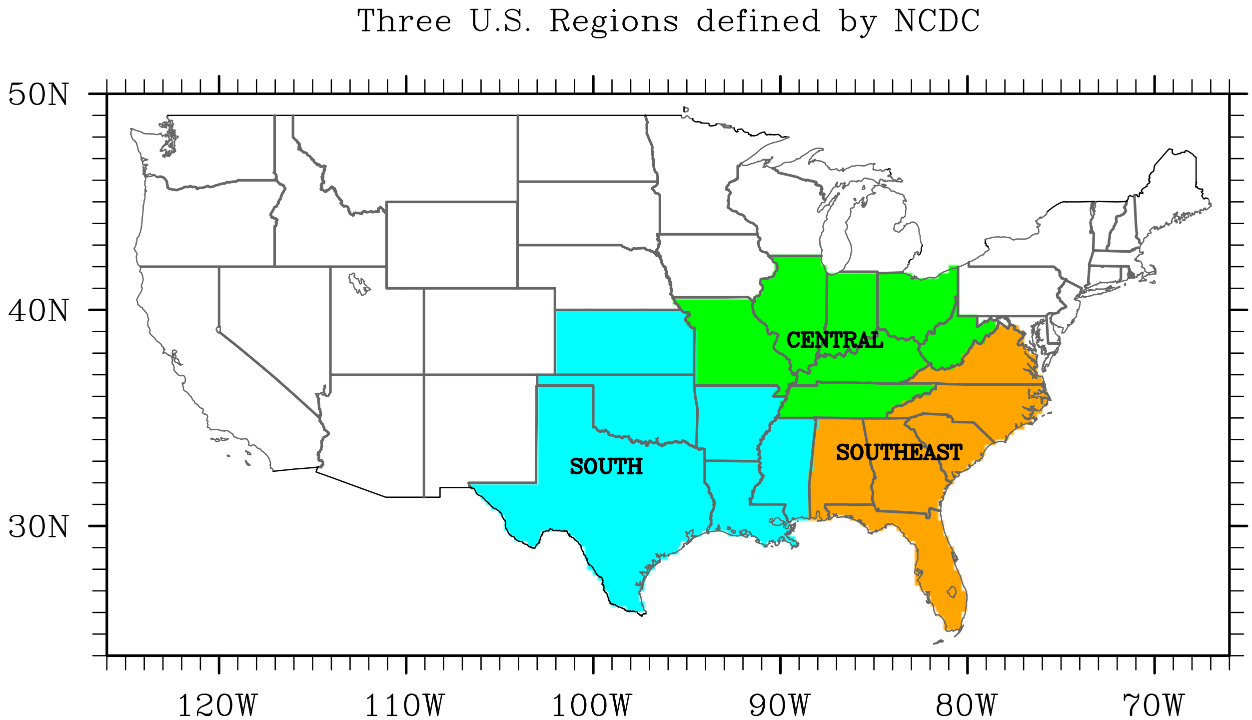

Figure S3. Three U.S. regions, namely the South, Central and Southeast, defined by National Climate Data Center. These regions are frequently referred in the main text to describe regional rainfall anomalies in the U.S.

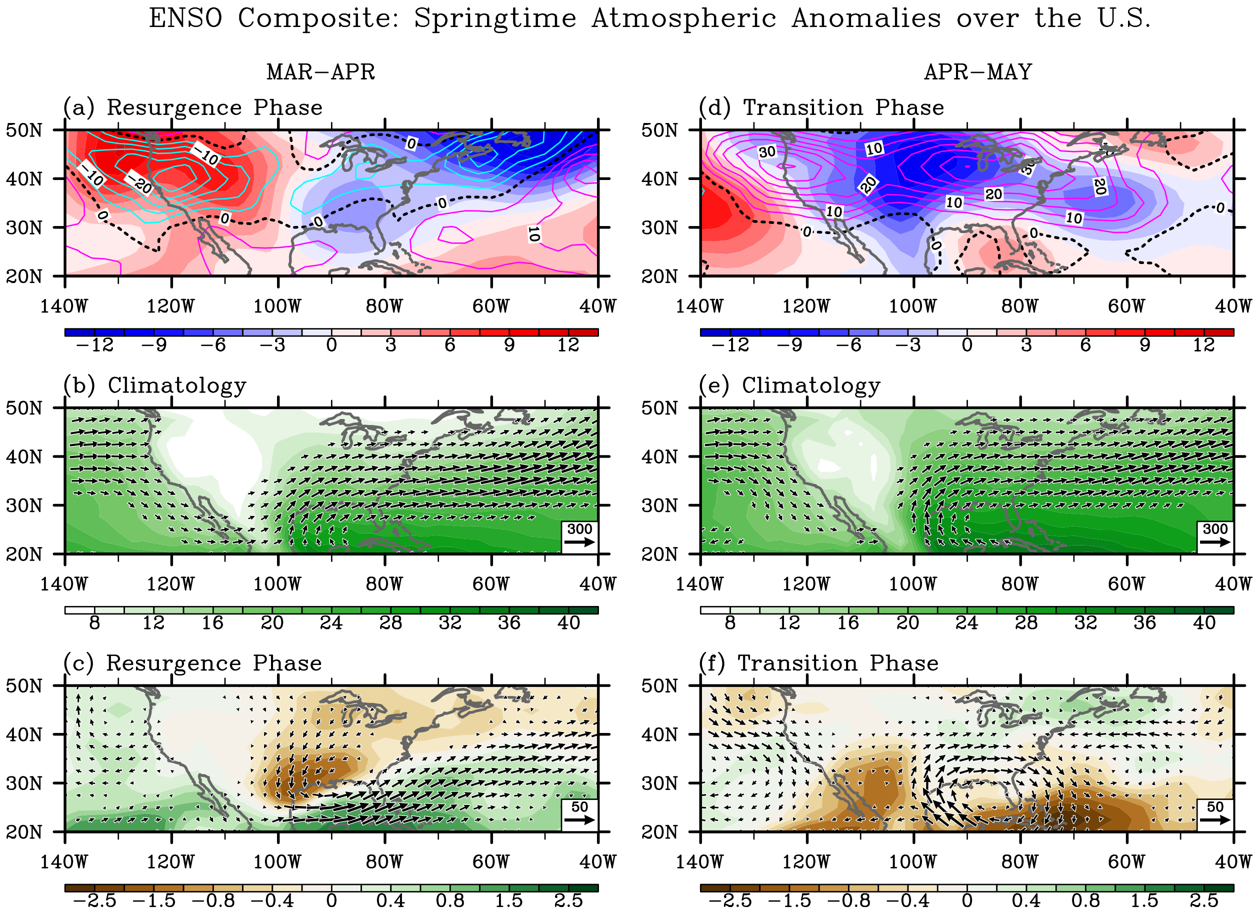

Figure S4. Upper-panel: anomalous geopotential height at 850 hPa (color shades) and variance of 5-day high-pass filtered meridional winds at 300 hPa (contours) for (a) early spring of ENSO resurgence phase and (d) late spring of ENSO transition phase. Mid-panel: climatological moisture transport (vectors) and precipitable water (color shades) in (b) early and (e) late spring. Bottom-panel: anomalous moisture transport (vectors) and precipitable water (color shades) for (c) early spring of ENSO resurgence phase (0.5 × [<El Niño resurgence> - <La Niña resurgence>]) and (f) late spring of ENSO transition phase (0.5 × [<El Niño-to-La Niña transition> - <La Niña-to-El Niño transition>]). The units are $kg{\cdot}m^{-1}{\cdot}s^{-1}$ for moisture transport, $kg{\cdot}m^{-2}$ for precipitable water, gpm for geopotential height and $m^2{\cdot}s^{-2}$ for variance of meridional winds.